Preparation and Characterization of Nanofibers Containing Amorphous Drug Dispersions Generated by Electrostatic Spinning

Geert Verreck,[1] Iksoo Chun,[2] Jef Peeters,[1] Joel Rosenblatt,[2] and Marcus E. Brewster[1,3]

Received December 16, 2002; accepted February 4, 2003

Purpose. We assessed the application of water-soluble polymer-based nanofibers prepared by electrostatic spinning as a means of altering the dissolution rate of the poorly water-soluble drug, itraconazole.
Methods. Organic solvent-based solutions of itraconazole/HPMC mixtures were electrostatically spun at 16 and 24 kV. The formed nanofibers were collected as a non-woven fabric. The samples were analyzed by scanning electron microscopy, differential scanning calorimetry, and dissolution rate.
Results. Scanning electron microscopy showed fiber diameters of 1–4 μm and 300–500 nm depending on the applied voltage. Differential scanning calorimetry measurements found that the melting endotherm for itraconazole was not present, suggesting the formation of an amorphous solid dispersion or solution. Dissolution studies assessed several presentations including direct addition of the nonwoven fabrics to the dissolution vessels, folding weighed samples of the materials into hard gelatin capsules and placing folded material into a sinker. Controls included a physical mixture as well as solvent cast and melt extruded samples. Electrospun samples dissolved completely over time with the rate of dissolution depending on the formulation presentation and drug to polymer ratio. The physical mixture did not appreciably dissolve in these conditions.
Conclusions. The application of electrostatic spinning to pharmaceutical applications resulted in dosage forms with useful and controllable dissolution properties.

KEY WORDS: electrostatic spinning; amorphous solid dispersion; itraconazole; improved dissolution rate.

INTRODUCTION

The inability to configure adequately bioavailable solid oral dosage forms for poorly water-soluble drug candidates is a significant impediment to their development. It has been estimated that almost 40% of all drug development failures are related to poor biopharmaceutical properties, including poor bioavailability associated with low drug solubility (1). Unfortunately, the nature of drug candidate identification techniques, especially high-throughput receptor screening, tends to select for compounds with high molecular weights, high lipophilicities, and poor water solubilities, meaning methods for improving drug solubility or dissolution rate continue to be highly sought after (2,3). Generally, the search for such methods have been guided by the Noyes–Whitney equation (4,5), which defines dissolution rate (dC/dt) as follows:

$$\frac{dC}{dt} = \frac{D \times A \times (C_s - C_t)}{h \times V}$$

where D is the diffusion coefficient, h, the diffusion layer thickness at the solid–liquid interface, A, the surface area of drug exposed to the dissolution media, V, the volume of the dissolution media, C_s, the saturation solubility of the drug, and C_t, the drug concentration at time, t. That is, dissolution rate can be increased by increasing the surface area of the drug (via micro- or nanosizing), by decreasing the diffusional layer thickness (through improving wettability by, e.g., addition of surfactants), and by altering the solubility of the drug (through formation of supersaturated drug solution via solid dispersion, complexation approaches, or by manipulation of the solid form to give more soluble salts, polymorphs, or amorphous material). As the water solubility of a drug decreases, the number of suitable options also becomes smaller. The development of a bioavailable formulation of itraconazole is a useful example. This broad-spectrum antifungal agent is a highly lipophilic (log p > 5) weak base (pKa ~4) with an aqueous solubility at neutral pH estimated at about 1 ng/mL (6–9). Other physicochemical properties are listed in Table I. The chemical structure is shown in Fig. 1.

After exploring numerous options including alternative salt forms, prodrugs, particle size reduction (even at nanometer dimensions) and use of surfactants, the only useful approaches for generating bioavailable solid oral dosage forms were those that gave rise to stable supersaturated solutions (10–13). Conversely, liquid dosage forms (intravenous and oral) could be prepared, developed, and marketed using complexation approaches with hydroxylpropyl-β-cyclodextrin serving as the functional excipient (9). Thus, the marketed solid oral capsule product is made up of a coated inert sugar sphere in which the coating is a solid solution containing itraconazole and hydroxylpropylmethylcellulose (HPMC) (14). As this thin film dissolved in water or gastric fluid, the molecularly dispersed itraconazole is released at supersaturated concentration with the co-dissolving HPMC acting as a stabilizer (i.e., to inhibit recrystallization of itraconazole). The supersaturated solutions of itraconazole are sufficiently stable to allow for absorption and distribution. An extension of the capsule-based systems, which essentially used solvent casting to form the solid solution, was the application of melt processing. Two methods were assessed including melt compression for small-scale application and melt extrusion as a potentially scaleable technique. In this case of melt extrusion, itraconazole and HPMC were processed followed by milling of the extrudate and pressing of the glassy powder into tablets with additional excipients (15). The melt-extruded tablets were also highly orally bioavailable. Given the success of these two types of processes, other techniques were considered. An attractive possibility was to try to combine solid solution/dispersion technology with nanotechnology. One polymer processing approach that may serve this purpose is electrostatic spinning (16,17). This versatile technique has been applied to various micro/nanofabrication areas using numerous polymers but very few uses in the pharmaceutical area have been reported (18,19). The technique involves sub-

[1] Johnson & Johnson Pharmaceutical Research and Development, Turnhoutseweg 30 2340, Beerse, Belgium.
[2] Johnson & Johnson Corporate Center for Biomaterials and Advanced Technologies, Somerville, New Jersey.
[3] To whom correspondence should be addressed. (e-mail: mbrewste@prdbe.jnj.com)

0724-8741/03/0500-0810/0 © 2003 Plenum Publishing Corporation

Table I. Physicochemical Characteristics of Itraconazole

MW	705.64
Partition coefficient	Log P > 5
Ionization constant	4.0
Melting point	166°C
Solubility in water (pH 7)	~1 ng/mL
Solubility in 0.1 N HCl	6 μg/mL

jecting a liquid stream of a drug/polymer solution to a potential of between 5 to 30 kV. As described by Reneker and Chun (16), fibers at submicron diameters can be formed when electrical forces overcome the surface tension of the drug/polymer solution at the air interface (termed a Taylor cone) such that a jet forms. As the jet accelerates through the electric field, two possible outcomes have been hypothesized, including 1) radial forces become increasingly important leading to a splaying of the solution stream or 2) a continuous, single filament is generated based on bending instability (20–22). As the solvent evaporates, the formed fiber(s) can be collected on a screen to give a non-woven fabric or collected on a spinning mandril. The fiber diameter is a function of the solution surface tension, the polymer solution dielectric constant, feeding rate as well as the electric field strength (22). The nature of the polymer can also direct the use of the electrospun fibers with water-soluble polymers giving rise to immediate release dosage forms and water-insoluble (i.e., biodegradable or nonbiodegradable) polymers being useful for sustained release systems (19). Thus, the fabrics generated with water-soluble carriers could be used in oral dosage formulations by direct incorporation of the materials into a capsule or by further processing (i.e., milling of the fabrics). Topical (i.e., wound healing) and other applications of these solid dispersions have also been suggested (19,23). The goal of the present communication was to assess the use of electrostatic spinning as a means of preparing solid solution or dispersions for a poorly water-soluble model compound (itraconazole) in a water-soluble polymer. In addition, the study was designed as to assess what the properties of the electrospun fabrics were relative to other solid solution/dispersion techniques such as melt-extrusion and solvent casting with regard to drug dissolution behavior.

MATERIALS AND METHODS

Itraconazole (purity more than 99%) was provided by Janssen Pharmaceutica (Beerse, Belgium) and hydroxypropylmethylcellulose 2910, 5 mPa (HPMC) was obtained from Aqualon, Hercules (Zwijndrecht, the Netherlands). Ethanol and methylene chloride were purchased from Aldrich Chemical Company and were used without further purification.

Electrostatic Spinning

The electrostatic spinner used for the experiments was equipped with a Spellman High Voltage DC Supply (Model No: RHR30PN30, Spellman High Voltage Electronics Corporation, Hauppauge, NY, USA). The applied voltage was set at either 16 or 24 kV. The distance between the spinneret and the fiber collector was mechanically controlled to 13 cm. The experiments were performed at ambient temperature and humidity. Physical blends containing 20% w/w and 40% w/w itraconazole, respectively, were obtained by mixing the drug with HPMC in a Turbula mixer for 10 min (Willy A. Bachhofen, Basel, Switzerland). Solutions were obtained by dissolving 12% w/w of the physical blends in a mixture of ethanol and methylene chloride (40/60 w/w). The solution was placed into the spinneret and a high voltage was applied to the drug/polymer solution. Upon completion of the spinning process, the non-woven electrostatically spun fabric was removed from the collector and either characterized as such or further milled prior to analysis.

Milling

The nonwoven fabric containing 40% w/w itraconazole was milled for 10 min using a cryogenic mill (Type 6750 Freezer/Mill, SPEX Certiprep Inc., Metuchen, NJ, USA). Cooling of the fabric during the milling process was performed using liquid nitrogen. The average fiber length after milling was about 27 μm.

Scanning Electron Microscopy (SEM)

The surface topography of the electrostatic spun fibers was assessed using a scanning electron microscope (JSM-5900LV, Japan Electron Optics Laboratory LTD). Electrostatically spun fibers were placed in the center of an aluminum stud. These fibers were fixed to the stud using liquid graphite conductive adhesive 154 (Electron Microscopy Sciences, PA, USA). A very thin layer of gold was applied to the fibers by a sputtering unit (EMS 550, Electron Microscopy Sciences, PA, USA). Gold-coated fibers were placed in the microscope chamber to which a high vacuum was applied.

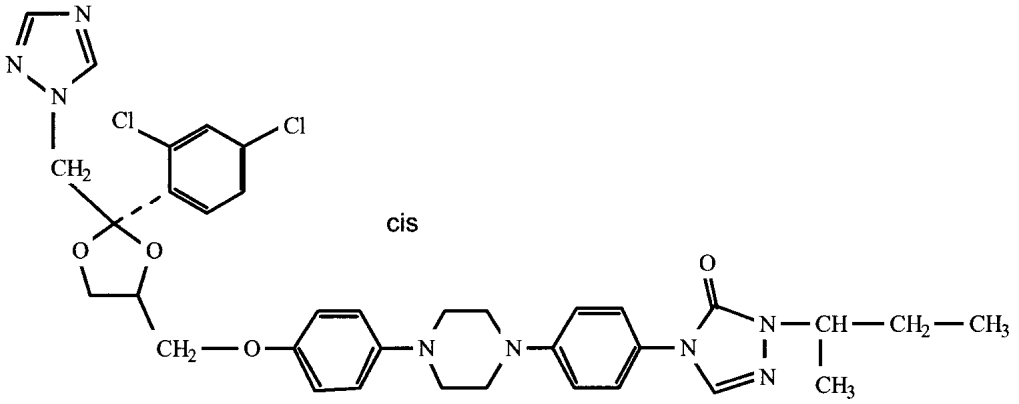

Fig. 1. Chemical structure of itraconazole

Surface morphologic features were obtained in 5–10 kV, usually 5 kV mode.

Differential Scanning Calorimetry (DSC)

The DSC measurements were performed using a Perkin–Elmer DSC-7 differential scanning calorimeter with a TAC7/DX thermal analysis controller. Cooling was provided with a Perkin–Elmer refrigerated cooling device (FC-60-PED). Data were treated mathematically using the resident Pyris Software. Calibration was conducted using indium and zinc as reference materials. The samples were analyzed in perforated and covered Aluminum pans under a Nitrogen purge. Approximately 5 mg of crystalline itraconazole was heated from 25 to 200°C with a heating rate of 20°C/min, and afterwards cooled with a cooling rate of 20°C/min to room temperature. A second heating cycle was then applied on the sample starting at room temperature up to 200°C with a heating rate of 20°C/min. In separate experiments, approximately 10 mg of HPMC 2910 5 mPa was heated from 25 to 200°C with a heating rate of 20°C/min. For the electrospun material, approximately 5 mg were weighed in the DSC pan. Both the unmilled and the milled sample were measured. The samples were heated from 25 to 200°C with a heating rate of 20°C/min.

In Vitro Drug Release Measurement

The dissolution of the nonwoven fabric was measured directly, manually filled into a hard gelatin capsule size 0 (Capsugel, Morris Plains, NJ, USA), or manually folded and filled in a sinker (metal spiral to enclose the sample and keep it submerged). The milled samples were measured directly and manually filled into a hard gelatin capsule size 0. The electrostatically spun samples were maintained at a drug dose of 50 mg. Dissolution measurement was performed in 600 mL of 0.1 N HCl (37°C) using a paddle rotating at 100 rpm (USP II apparatus). Samples were taken at predetermined time intervals up to 24 h. An aliquot of 3 mL was filtered through a Millex HV 0.45-μm filter (Millipore SLHV R04 NL) with the removed solvent not being replaced with fresh solvent. The concentration of itraconazole was quantified with UV at a maximum wavelength of 254 nm. For comparison, a physical mixture, a solvent-cast film and a melt-extruded sample of itraconazole and HPMC 40/60 w/w were also assayed.

Preparation of a Solvent Cast Film

A solvent cast film of itraconazole and HPMC was prepared by dissolving the ingredients in a mixture of ethanol and methylene chloride 20/80 v/v in a drug/polymer ratio of 40/60 w/w. The solvent was evaporated in a vacuum oven at 80°C for 1 h. Samples containing 100 mg of drug were directly added to 300 mL of simulated gastric fluid (without pepsin; 37°C) and dissolution was assessed using a paddle rotating at 100 rpm (USP II apparatus).

Preparation of Melt Extruded Samples

A melt-extruded sample was prepared using a co-rotating twin-screw extruder APV MP19 PH 25:1 (APV, UK). The screw configuration consisted of two mixing zones and three transporting zones over the barrel length. The barrel contained 5 heating zones. In the experiment, the temperature of the heating zones was adjusted to 25, 150, 200, 220, and 220°C, respectively. The physical mixture was fed into the extruder at 2 kg/h by a gravimetric feeder (K-Tron, UK) and was melted throughout the barrel at a screw speed of 300 rpm. At the exit of the barrel, a die plate was installed containing one orifice (diameter 3 mm). The extrudated strands were cooled at ambient temperature on a conveyer belt. The strands were milled with an IKA M20 universal laboratory mill (IKA-Werke GmbH&Co, Staufen, Germany) and sieved to obtain a particle size fraction below 150 μm. Samples with a 200 mg dose were directly added to 900 ml of 0.1 N HCl (37°C) and dissolution was assessed using a paddle rotating at 150 rpm (USP II apparatus).

RESULTS AND DISCUSSION

Nanofiber-based nonwoven fabrics could be obtained using drug/polymer solutions at a concentration of 12% w/w (drug in solvent) in ethanol/methylene chloride (40/60 w/w). This concentration proved to be optimal since at higher values (15% w/w), the viscosity of the solution became limiting while at lower concentrations (10% w/w), nanofiber could not be formed due to "sputtering" of the solution. The molecular weight and the viscosity of the prepared drug/polymer solution determine the optimal polymer concentrations for electrostatic spinning. Kenawy *et al.* found that for polylactic acid (PLA), poly(ethylene-co-vinyl acetate) (PEVA), and mixtures of the two could be spun (out of a chloroform solution) at 14% w/v concentration (18). Ignatious *et al.* found that polyethylene oxide (Polyox) could be spun out of aqueous acetonitrile at concentrations ranging from 2.5–30% w/v based on the grade and molecular weight (100,000 to 7,000,000 d) of the polymer (19). Working with aqueous solutions of polyethylene oxide at a MW of 1,450,000 Da, Doshi and Reneker found that electrostatic spinning was most efficient between a solution viscosity of 800 to 4000 centipoise (17).

SEM was used to determine the morphology of the spun fibers and the formed non-woven fabrics. As illustrated in Fig. 2 (spinning at 16 kV), fibers were generated with diameters of 1 to 4 μm when a 40:60, itraconazole:HPMC ratio was used. Increasing the potential to 24 kV resulted in a reduction of the fiber diameter, which was estimated at approximately 300

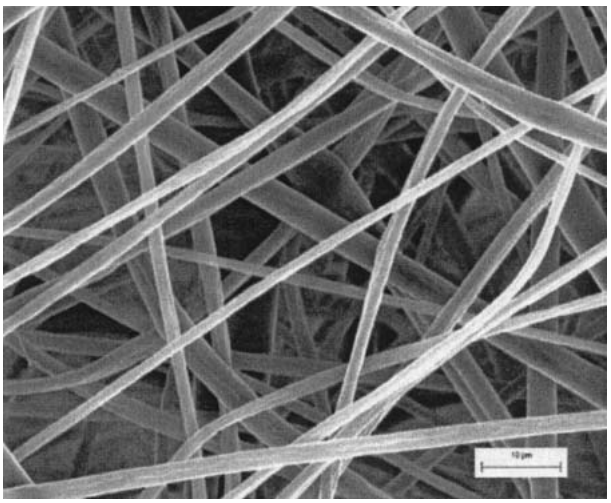

Fig. 2. Scanning electron micrograph (magnification 2000×) of itraconazole/HPMC 40:60 w/w electrostatically spun fibers at 16 kV.

to 500 nanometers for this same drug/polymer ratio (Fig. 3). Spinning of a itraconazole:HPMC (20:80) solution (12% w/w) across a 24-kV potential also resulted in the formation of cylindrical fibers but these tended to be more variable in diameter. As shown in Fig. 4, the material produced could be characterized with fibers ranging from 500 nm to 3 μm. These results indicate that the applied voltage and drug/polymer ratios can have an impact on the fiber diameter. These data are similar to those generated for non-water soluble polymers. PEVA and PLA-PEVA blends (50:50), for example, generated fibers of between 1–3 μm when spun across a potential of 15 kV of a 14% w/v solution while PLA alone generated larger fibers (3–6 μm) under similar conditions (18). Polymeric fabrics prepared by this method have similar macroscopic properties including opacity (as a function of light scattering) although mechanical properties are related both to the processing method as well as the polymer used for the spinning (19). The micro/nanostructure of the materials appear to be process and polymer-dependent. SEM micrographs suggest that fabrics generated from HPMC generate more regular and less interconnecting matrices while those of PLA/PEVA are more "matted" in appearance (18). Micrographs of highly drug loaded Polyox tended to show the greatest extent of fiber diameter heterogenicity with the highest branched morphology (19).

Because the fiber diameters are at the nano to microrange, a large specific surface area is obtained resulting in fast and efficient evaporation of the organic solvent. As a result of the rapid rate of solvent evaporation, the possibility of forming noncrystalline solid dispersions or solid solutions is favored because the drug/polymer system has limited time to recrystallize. The ability of compounds to form solid solutions or amorphous dispersions is, of course, also a function of intrinsic properties of the candidate molecules as well as interaction of these compounds with the specific polymers used in the nanofiber formation. DSC was performed to determine the physical form of the model drug, itraconazole, in the nonwoven nanofibrous mats as well as of the unmanipulated materials. The thermogram of crystalline itraconazole shows an endothermic melting peak with its maximum at 172°C (T_m) and an enthalpy (ΔH) of melting of about 85 J/g. During cooling of the melt, two exothermic peaks (T_c) are observed at 87°C and 69°C, respectively, both of which are associated with small enthalpies. Reheating these samples results in a glass transition (T_g) at 60°C and two endothermic peaks at 76°C and 92°C, respectively, characterized by a low enthalpy. It has been suggested by Six *et al.* (24) that the transitions observed during the cooling and the second heating run of itraconazole represent the formation of glassy itraconazole and a monotropic mesophase upon cooling from the melt. HPMC shows a glass transition at 141°C. Figure 5 gives the DSC profiles of the electrostatically spun samples. Both unmilled samples lack a melting peak as well as the thermal events related to monotropic mesophase formation for itraconazole. These results suggest that electrostatic spinning produces an amorphous solid dispersion of itraconazole and HPMC (12). The milled sample shows two endothermal events: a large endotherm due to solvent loss (60 to 115°C) and a small endothermic peak at 163°C with an enthalpy of about 1.4 J/g. This latter small endotherm probably represents the presence of a small amount of recrystallized itraconazole (4.1% based on ΔH calculation), which was likely induced by the milling process.

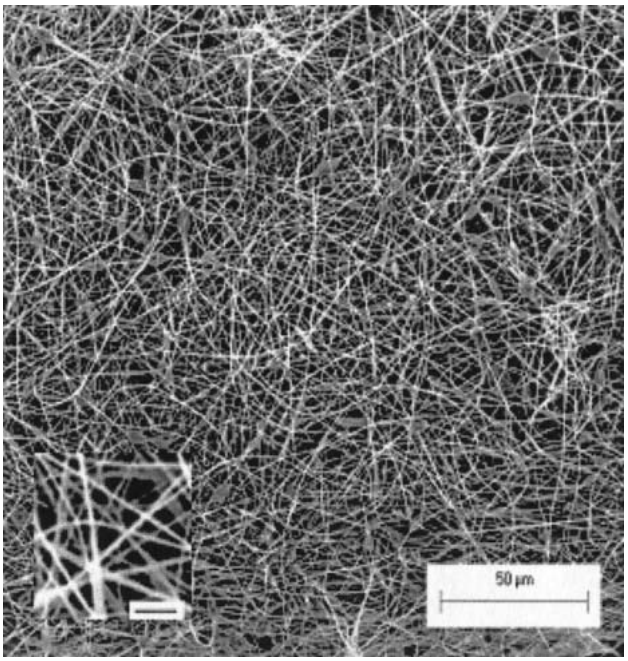

Fig. 3. Scanning electron micrograph (magnification 500×) of itraconazole/HPMC 40:60 w/w electrostatically spun fibers at 24 kV. In the insert (magnification 8500×), the bar represents 3 μm.

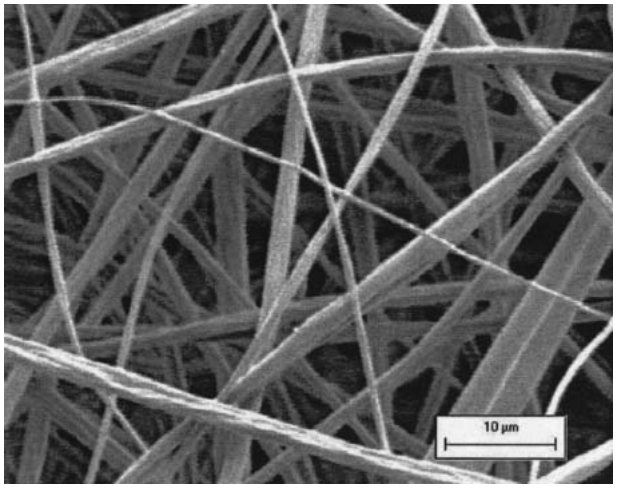

Fig. 4. Scanning electron micrograph (magnification 2000×) of itraconazole/HPMC 20:80 w/w electrostatically spun fibers at 24 kV

All electrostatically spun samples have a glass transition between 60°C and 80°C (exact values not shown). The theoretical value for the T_g of a binary mixture (assuming ideal mixing) can be calculated using the Gordon–Taylor/Kelly–Bueche equation (25,26)

$$Tg_x = \frac{Tg_1 w_1 + Tg_2 K w_2}{w_1 + K w_2}$$

in which Tg_1 and Tg_2 are the glass transition temperature of HPMC (141°C) and itraconazole (60°C), respectively, w_1 and w_2 are the weight fractions of HPMC and itraconazole in the dispersions, respectively, and K is a constant which can be calculated using the Simha–Boyer rule (27):

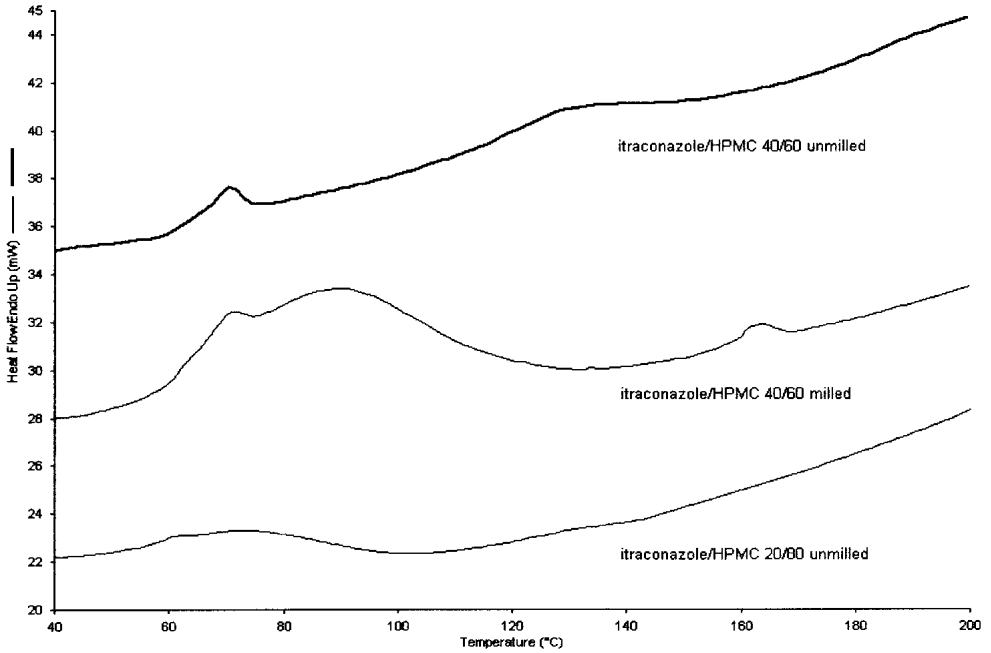

Fig. 5. Differential scanning calorimetry profiles of electrostatic spun samples (at 24 kV) of itraconazole/HPMC 40:60 unmilled and milled and itraconazole/HPMC 20:80 unmilled. The samples were heated from 25°C to 200°C with a heating rate of 20°C/min in perforated and covered aluminum pans under a nitrogen purge.

$$K \cong \frac{\rho_1 Tg_1}{\rho_2 Tg_2}$$

where ρ is the density of the amorphous solid. Although the Gordon–Taylor relationship was originally derived for compatible polymer blends, it has been used successfully applied to small organic molecules. Using these relationships for the itraconazole/HPMC systems, theoretical values for the 40:60 w/w and 20:80 w/w binary dispersion can be calculated as 108°C and 125°C respectively. It is clear from the DSC profiles that the measured T_g deviates from the calculated values, indicating either phase separation (i.e., an amorphous dispersion) or drug–polymer interactions and not the formation of a solid solution.

As overviewed by Kissel *et al.* for drug-loaded polymeric particles (28), at least three morphologies are possible, including 1) systems where the drug is dissolved at the molecular level, i.e., solid solution, 2) systems where the drug is distributed in the polymer matrix as either crystalline or amorphous aggregates, i.e., solid dispersions, or 3) systems where the drug phase separates generating a more or less crystalline drug core surrounded by polymer layer, i.e., a micro/nanocapsule. These classifications may also be applied to drug-containing polymeric nanofibers. The data generated above suggest that an amorphous nanodispersion of itraconazole is generated in the polymer matrix. Other systems generate other constructs. Spinning of tetracycline hydrochloride in PLA, PEVA, or PLA/PEVA mixtures produces nanofibers with crystalline drug present in and on the fibers as indicated by SEM analysis (18). DSC analysis of nanofibers prepared with nabumetone and Polyox indicated that no crystalline drug was present at drug loadings of 30% and lower while melting endotherms of the drug were evident at drug loading greater than 30% (19). These data are suggestive of either an amorphous dispersion or solid solution.

The release profiles of itraconazole from an itraconazole/HPMC 40:60 w/w electrostatic spun fabric were shown as a function of the applied voltage and formulation presentation in Fig. 6. When fabric spun at either 16 or 24 kV is added directly to the dissolution medium, complete release is observed for both although there is a tendency for the material spun at 16 kV (i.e., the larger fiber diameter) to release itraconazole faster than the fibers spun at 24 kV (i.e., the smaller fibers). At 60 min, for example, 40% release of itraconazole is observed in the 24-kV sample whereas 70% release is seen in the case of the 16 kV sample. Complete release is obtained at ~160 min for the 16 kV sample and by 240 min for the 24 kV material. The difference in release rates could not be explained by thermal characterization since the thermograms of both samples (i.e., those spun at 16 and 24 kV) were closely related to one another with similar glass transitions and solvent loss events as well as the absence of a melting peak for itraconazole. One speculation is that the differences in dissolution rates may be related to wettability and solvent accessibility between the tightly packed 300–500 nm fiber-based fabric and the more loosely packed 1-4 μm non-woven material. When the non-woven material is folded and placed either in a sinker or hard gelatin capsule, significantly longer dissolution times are generated (i.e., release times of 24 h or greater). In the case of the capsules, there was a tendency for the 24 kV samples to release drug faster than the 16 kV regimens. For example, the 24 kV-produced fabric loaded into hard gelatin capsules released ~65% of the itraconazole load by 500 min compared with ~45% release for the 16 kV sample. The importance of this reversed order of release as a function of formulation and fiber diameter (i.e., fabric added directly to the dissolution bath vs. fabric folded and placed in a gelatin capsule and 300–500 nm vs. 1–4 μm fibers) is interesting but, again, not explained by the available thermoana-

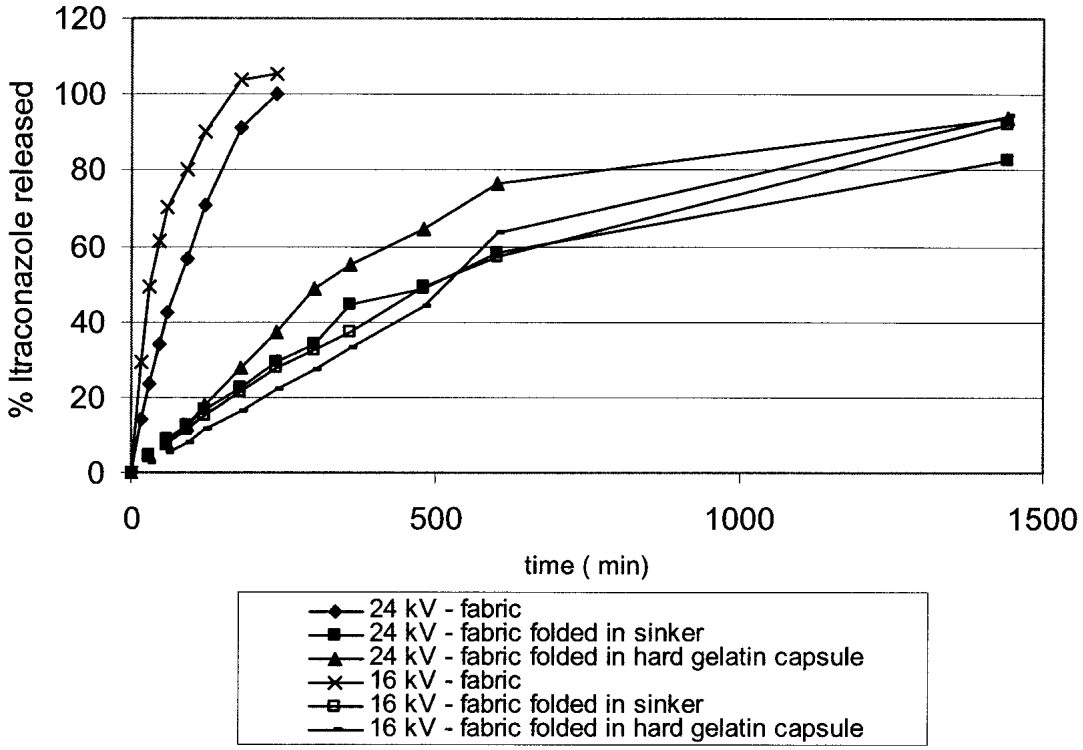

Fig. 6. *In vitro* drug release of itraconazole/HPMC 40:60 w/w electrostatic spun fabrics as a function of the applied voltage (16 kV vs. 24 kV) and method of measurement (directly vs. sinker vs. hard gelatine capsule). Samples with a 50 mg dose were added to 600 mL of 0.1 N HCl (37°C) and dissolution was assessed using a paddle rotating at 100 rpm (USP II apparatus).

lytical evidence. As suggested for the 16 and 24 kV spun materials, these results may be related to differential dissolution and wetting of the encapsulated vs. the non-encapsulated electrospun fabric. The effect of drug/polymer ratio on the *in vitro* release characteristics of itraconazole/HPMC electrostatic spun fabrics is shown in Fig. 7. In this set of comparisons, there tended to be little effect of the polymer-drug ratio for fabric added directly to the dissolution bath. For the hard gelatin capsule and sinker systems, there was a clear trend that a higher polymer to drug relationship resulted in a greater rate or extent of itraconazole release. These effects may reflect the nature of the encapsulation. In the sinker or the hard gelatin capsule, wettability is reduced and the possibility for agglomeration is increased. This can alter the ability of the dissolution media to discriminate between the prototypical dosage forms. The effect of milling on the release of itraconazole/HPMC 40:60 w/w electrostatic spun fabrics is demonstrated in Fig. 8. Milling tended to reduce the rate and extent of drug release especially in the case where the fabrics were added directly to the dissolution bath. The DSC measurements indicated that the milled samples contained small amounts of crystalline itraconazole and the *in vitro* drug release did appear to be affected by the presence of these trace amounts of crystalline drug. Importantly, the absolute value of the differences in dissolution rates was small. The release of itraconazole/HPMC 40:60 w/w binary dispersions obtained by different preparation methods: physical mixture, solvent casting, melt extrusion and electrostatic spinning, were examined. Even though the dissolution methods varied for the different presentations, several apparent trends were observed. Simple physical mixtures of itraconazole and HPMC generated very little (<1–3%) drug release in any of the dissolution approaches assessed. Solvent casting and melt extrusion of itraconazole and HMPC have been shown to generate solid solutions or amorphous drug dispersions (15,29–31). Both processing techniques result in samples that rapidly released itraconazole with the solvent cast film giving more complete release in these experiments. Samples produced using electrostatic spinning resulted in a complete *in vitro* release over time, but the dissolution rate was slower than for either the cast thin films or the melt extruded, milled powder.

These dissolution results differ from those associated with electrostatically spun fibers of low water solubility and from systems in which the drug is dispersed in a crystalline form. In the case of PLA, PEVA, or PLA/PEVA blends and tetracycline hydrochloride, significant bursts were observed presumably because of the dissolution of crystalline drug substance present on the fiber surfaces (18). For PLA, there was little or no second phase drug release over a time course of hours, suggesting that the partial crystallinity of the PLA polymer trapped internalized tetracycline and the time course was too short to see polymer erosion. For PEVA and the PEVA/PLA blends, sustained drug release phases were obtained so long as the drug loading was low (i.e., 5%). These systems were superior to simple cast films of the water insoluble polymers where again a burst phase with minimal subsequent drug release were observed.

CONCLUSIONS

These results indicate a number of potential applications of electrostatically spun fibers in drug delivery based on the

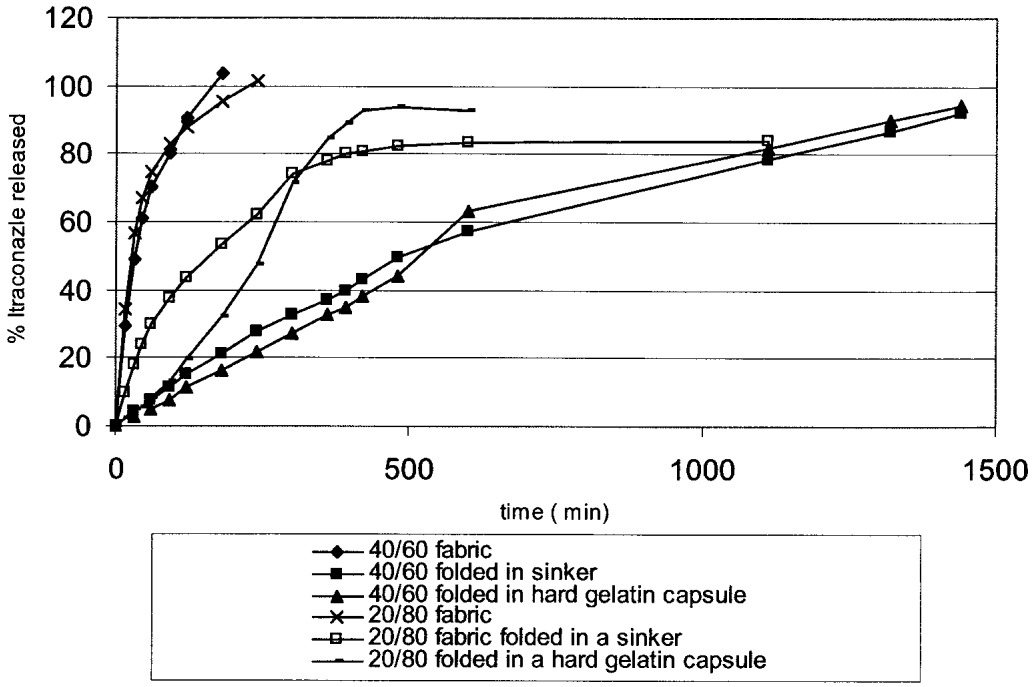

Fig. 7. *In vitro* drug release of itraconazole/HPMC electrostatic spun fabrics (spun at 24 kV) as a function of drug/polymer ratio (40:60 vs. 20:80) and method of measurement (directly vs. sinker vs. hard gelatin capsule). Samples with a 50 mg dose were added to 600 mL of 0.1 N HCl (37°C) and dissolution was assessed using a paddle rotating at 100 rpm (USP II apparatus).

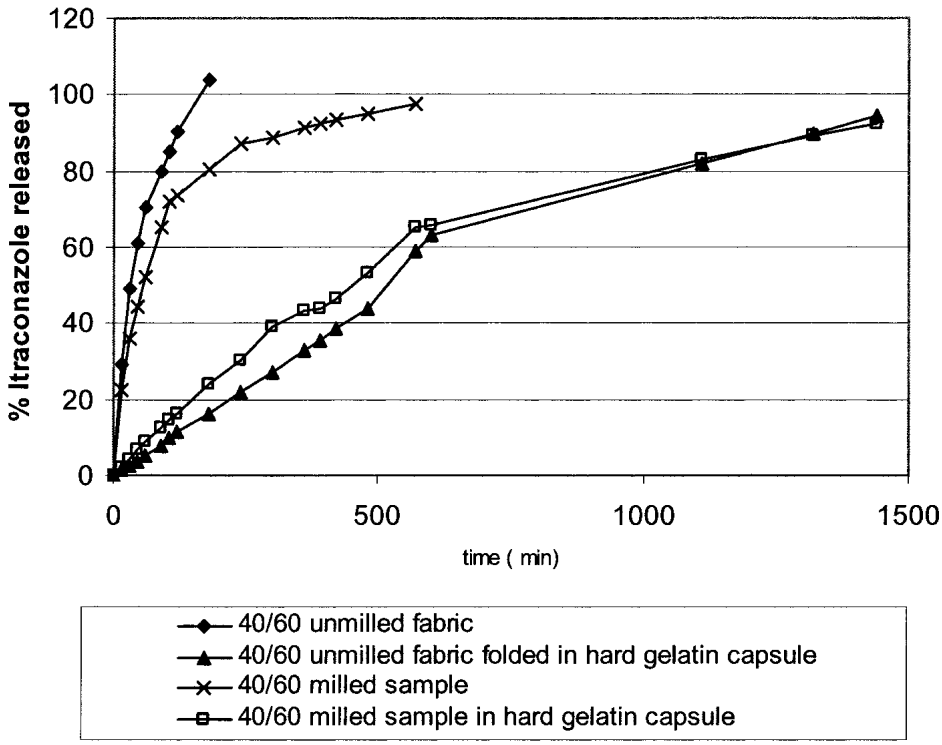

Fig. 8. *In vitro* drug release of itraconazole/HPMC 40:60 w/w electrostatic spun fabrics (spun at 24 kV) compared to a milled sample (directly vs. hard gelatine capsule). Samples with a 50 mg dose were added to 600 mL of 0.1 N HCl (37°C) and dissolution was assessed using a paddle rotating at 100 rpm (USP II apparatus).

following observations: 1) complete release of highly poorly water-soluble drugs can be achieved and 2) the rate of drug release can be tailored. Specifically, drug release can be controlled by a variety of parameters: for example, the drug/polymer ratio, the diameters of the electrospun fibers and the presentation used (nonwoven fabrics, folding samples of the materials into hard gelatin capsules (size 0), folding material into a sinker, milling). This suggests that electrostatic spinning can be used for the difficult task of controlled drug delivery for poorly water-soluble drugs in addition to other applications such as wound healing, buccal applications and topical applications.

REFERENCES

1. R. A. Prentis, Y. Lis, and S. R. Walker. Pharmaceutical innovation by seven UK-owned pharmaceutical companies (1964-1985). *Br. J. Clin. Pharmacol.* **25**:387–396 (1988).
2. C. A. Lipinski, F. Lombardo, B. W. Dominy, and P. J. Feeney. Experimental and computational approaches to estimate solubility and permeability in drug discovery and development settings. *Adv. Drug Deliv. Rev.* **23**:3–25 (1997).
3. C. A. Lipinski. Avoiding investment in doomed drugs. *Curr. Drug Discov.* **1**:17–19 (2001).
4. A. A. Noyes and W. R. Whitney. The rate of solution of solid substances in their own solutions. *J. Am. Chem. Soc.* **19**:930–934 (1897).
5. D. E. Wurster and P. W. Taylor. Dissolution rates. *J. Pharm. Sci.* **54**:169–175 (1965).
6. S. M. Grant and S. P. Clissold. *Itraconazole. Drugs* **37**:310–344 (1989).
7. K. De Beule. and J. Van Gestel. Pharmacology of itraconazole. *Drugs* **61**(Suppl. 1):27–33 (2001).
8. S. Jain and V. Seghal. Itraconazole: an effective oral antifungal for onchomychosis. *Int. J. Dermatol.* **40**:1–5 (2001).
9. J. Peeters, P. Neeskens, J. P. Tollenaere, P. Van Remoortere, and M. E. Brewster. Characterization of the interaction of 2-hydroxypropyl-β-cyclodextrin with itraconazole at pH 2, 4 and 7. *J. Pharm. Sci.* **91**:1414–1422 (2002).
10. P. Sheen, V. Khetarpal, C. Cariola, and C. Rowlings. Formulation of a poorly water-soluble drug in solid dispersions to improve bioavailability. *Int. J. Pharm.* **118**:221–227 (1995).
11. A. T. Serajuddin. Solid dispersion of poorly water-soluble drugs. Early promises, subsequent problems and recent breakthroughs. *J. Pharm. Sci.* **88**:1058–1066 (1999).
12. C. Leuner. and J. Dressman. Improving drug solubility for oral delivery using solid dispersion. *Eur. J. Pharm. Biopharm.* **50**:47–60 (2000).
13. D. Erkoboni and R. Andersen. Improved aqueous solubility pharmaceutical formulation. World Patent 0056726 (2000).
14. P. A. Gilis, V. De Conde, and R. Vandecruys. Beads having a core coated with an antifungal and a polymer. US Patent 5633015 (1997).
15. L. Baert, D. Thone, and G. Verreck. Antifungal compositions with improved bioavailability. World Patent 9744014 (1997).
16. D. H. Reneker and I. Chun. Nanometre diameter of polymer, produced by electrospinning. *Nanotechnology* **7**:216–223 (1996).
17. J. Doshi and D. H. Reneker. Electrospinning process and applications of electrospun fibers. *J. Electrostatics* **35**:151–160 (1995).
18. E. R. Kenawy, G. L. Bowlin, K. Mansfield, J. Layman, D. G. Simpson, E. H. Sanders, and G. E. Wnek. Release of tetracycline hydrochloride from electrospun poly(ethylene-co-vinylacetate), poly(lactic acid), and a blend. *J. Control. Release* **81**:57–64 (2002).
19. F. Ignatious and J.M. Baldoni. Electrospun pharmaceutical compositions. World Patent 0154667 (2001).
20. A. L. Yarin, S. Koombhongse, and D. H. Reneker. Taylor cone and jetting from liquid droplets in electrospinning of nanofibers. *J. Appl. Phys.* **90**:4836–4846 (2001).
21. A. L. Yarin, S. Koombhongse, and D. H. Reneker. Bending instability in electrospinning of nanofibers. *J. Appl. Phys.* **89**:3018–3026 (2001).
22. J. M. Deitzel, J. Kleinmeyer, D. Harris, and N. C. Beck Tan. The effect of processing variables on the morphology of electrospun nanofibers and textiles. *Polymers* **42**:261 (2001).
23. D. S. Kath, K. W. Robinson, M. A. Attawia, F. K. Ko, and C. T. Laurencin. Bioresorbable nanofiber based systems for wound healing: optimization of fabrication parameters. Transactions of the 28th Annual Meeting for the Society for Biomaterials, 143 (2002).
24. K. Six, G. Verreck, J. Peeters, K. Binnemans, K. Bergmans, P. Augustijns, R. Kinget, and G. Van den Mooter. Investigation of thermal properties of glassy itraconazole: identification of monotropic mesophase. *Thermochim. Acta* **376**:175–181 (2001).
25. F. N. Kelley and F. Bueche. Viscosity and glass-transition temperature relations for polymer-dilute systems. *J. Poly. Sci.* **50**:549–556 (1961).
26. M. Gordon and J. S. Taylor. Ideal copolymers and the second-order transitions of synthetic rubbers. I. Noncrystalline copolymers. *J. Appl. Chem.* **2**:493–500 (1952).
27. R. Simha and R. F. Boyer. General relation involving the glass temperature and coefficients of expansion of polymers. *J. Chem. Phys.* **37**:1003–1007 (1962).
28. T. Kissel, M. A. Rummelt, and H. P. Bier. Wirkstoffreisetzung aus bioabbaubaren Mikropartikeln. *Dtsch. Apoth. Ztg.* **133**:29–32 (1993).
29. G. Verreck, L. Baert, J. Peeters, and M. Brewster. Improving aqueous solubility and bioavailability for itraconazole by solid dispersion approach. *AAPSPharmSci* **3**:M2157 (2001).
30. K. Six, C. Leuner, J. Dressman, G. Verreck, J. Peeters, N. Blaton, P. Augustijns, R. Kinget, and G. Van den Mooter. Thermal properties of hot-stage extrudates of itraconazole and Eudragit E100. Phase separation and polymorphism. *J. Thermal Anal. Calorimetry* **68**:591–601 (2002).
31. L. Baert, J. Peeters and G. Verreck. Solid mixtures of cyclodextrins prepared via melt-extrusion. World Patent 9718839 (1997).